



OPEN

Synthesis of benzylidenemalonitrile by Knoevenagel condensation through monodisperse carbon nanotube-based NiCu nanohybrids

Nursefa Zengin¹, Hakan Burhan², Aysun Şavk², Haydar Göksu^{1✉} & Fatih Şen^{2✉}

Monodisperse nickel/copper nanohybrids (NiCu@MWCNT) based on multi-walled carbon nanotubes (MWCNT) were prepared for the Knoevenagel condensation of aryl and aliphatic aldehydes. The synthesis of these nanohybrids was carried out by the ultrasonic hydroxide assisted reduction method. NiCu@MWCNT nanohybrids were characterized by analytical techniques such as X-ray diffraction (XRD), X-ray photoelectron spectroscopy (XPS), transmission electron microscopy (TEM), high-resolution transmission electron microscopy (HR-TEM), and Raman spectroscopy. According to characterization results, NiCu@MWCNT showed that these nanohybrids form highly uniform, crystalline, monodisperse, colloidally stable NiCu@MWCNT nanohybrids were successfully synthesized. Thereafter, a model reaction was carried out to obtain benzylidenemalonitrile derivatives using NiCu@MWCNT as a catalyst, and showed high catalytic performance under mild conditions over 10–180 min.

Benzylidenemalonitrile (BMN) derivatives are frequently used as both a target molecule and an intermediate molecule in organic chemistry. BMN derivatives have attracted many scientists' attention because of some unique properties such as anticancer^{1–3}, antifungal^{4,5}, antibacterial^{6–9}, anti-corrosive¹⁰. BMN derivatives are used to increase cell resistance in the case of oxidative stress¹¹, in prostaglandin biosynthesis¹², in the design of photoconductive cells¹³ and the inhibition/activation of certain enzymes^{14,15}.

Typically, BMN derivatives are synthesized by the Knoevenagel condensation of aldehydes with active methylene compounds (Fig. 1)^{16–22}. In these processes, it is seen that it has an effect on homogeneous catalysts. Heterogeneous catalysts have various advantages such as minimum availability, recovery, reusability, structural deterioration resistance and leaching of metal values^{23–28}. Bimetallic heterogeneous catalysts, in particular, have greatly facilitated the Knoevenagel condensation reaction^{29–34}. In literature, many catalysts such as SBA-15 (highly stable mesoporous silica)³⁵, Sr₃Al₂O₆ nanoparticles³⁶, bifunctional MIL-101(Cr)³⁷, Fe₃O₄@SiO₂ nanoparticles³⁸ and Mn-MOF@Pi³⁹ have been used in condensation reactions.

Herein we report an eco-friendly and practical method for the synthesis of highly efficient, cost-effective, and monodisperse bimetallic NiCu@MWCNT nanohybrids for the Knoevenagel condensation reaction under mild conditions. BMN derivatives have been successfully obtained in a very short time (10–180 min) using the developed method in the water-containing solvent system.

Experimental

Chemicals. NiCl₂, CuCl₂, NaBH₄, aminoborane aryl azides, acetonitrile (ACN), lithium perchlorate (LiClO₄), 3,4-ethylene dioxythiophene (EDOT), multiwall carbon nanotubes, NN-Dimethylformamide (DMF), sulfuric acid, hydrochloric acid, and nitric acid were purchased from Sigma-Aldrich. Tetrahydrofuran (THF; 99.5%), HClO₄ (60%), 2-propanol, and Methanol (≥99.5%) were obtained from Merck. All test materials and other

¹Kaynasli Vocational College, Duzce University, Düzce 81900, Turkey. ²Sen Research Group, Biochemistry Department, Faculty of Arts and Science, Dumlupınar University, Evliya Çelebi Campus, 43100 Kütahya, Turkey. ✉email: haydargoksu@duzce.edu.tr; fatih.sen@dpu.edu.tr

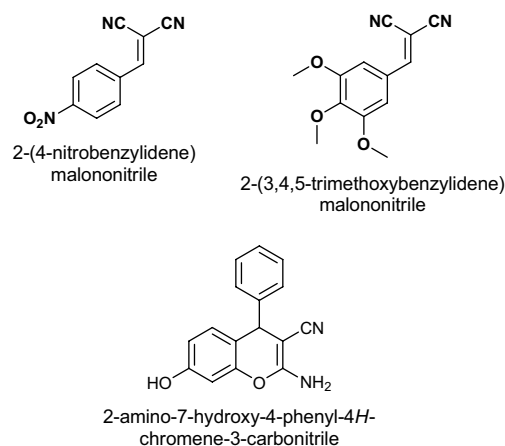


Figure 1. Benzylidenemalononitrile derivatives.

components were cleaned with distilled water. The pure water used was supplied by the Millipore water distillation system.

The preparation of monodisperse NiCu@MWCNT nanohybrids. NiCu@MWCNT nanohybrids were synthesized using the new ultrasonic hydroxide assisted descent method. 5.25 mg/mL MWCNT, 0.25 mmol CuCl_2 , and NiCl_2 precursors were combined in 20 mL water, followed by synthesis under an ultrasonic tip sonicator for 1 h. Finally, 20 mg of sodium borohydride solution was added. The generation of the monodisperse NiCu@MWCNT nanohybrids was observed with the formation of black color. The obtained NiCu@MWCNT nanohybrids were dried in a vacuum oven at 25 °C. Monodisperse NiCu@MWCNT nanohybrids were synthesized and characterized by Raman spectroscopy, XPS, TEM, HRTEM, and XRD techniques. After the characterization of nanohybrids, the catalytic performance of BMN derivatives was investigated.

Preparation and application of the Knoevenagel condensation studies of aryl and aliphatic aldehydes. 4 ml of water/methanol (1:1) solution containing 4 mg NiCu@MWCNT nanohybrids was placed in an ultrasonic bath for 30 s, and at room temperature 1.0 mmol of malononitrile and 1.0 mmol of aldehydes were transferred into the resulting solution (during stirring), and then the slurry was closed. During the mixing, the products formed in the reaction occurred were examined by thin-layer chromatography (TLC). The completion of the entire reaction time ended within 10–180 min, and centrifugation (7,500 rpm) was performed to remove the nanohybrid. The obtained nanohybrid was washed several times using water and methanol, dried in vacuum at room temperature. The purification of the solid sample was done using a chromatography system containing a ratio of 1:9 EtOAc/hexane. ^1H and ^{13}C NMR spectra were taken with deuterated solvents and products were determined using spectra.

Results and discussion

The morphology and metal nanoparticles distribution on the NiCu@MWCNT nanohybrids were investigated using HR-TEM and TEM analysis. Figure 2a reveals the uniform dispersion of nickel and copper on multiwalled carbon nanotube and homogeneous catalyst structure. The lattice fringe of the NiCu@MWCNT nanohybrids was investigated with HRTEM analysis. A lattice fringe of 0.21 nm corresponding to NiCu (111) was detected on the surface of NiCu@MWCNT nanohybrids. This value is very close to the nickel nominal value of 0.20. This smaller value of the atomic lattice fringe of NiCu nanohybrids compared to the nominal value can be explained by the alloy formation on the catalyst surface. Further, the average particle size of prepared nanohybrid was calculated by accounting for almost 100 particles and, a histogram was given in Fig. 2b. The average particle size of monodisperse NiCu@MWCNT nanohybrids was found to be 3.89 ± 0.41 nm.

The Raman analysis in Fig. S1a shows the ratio of the intensity of D-G bands (I_D/I_G) for NiCu@MWCNT nanohybrids and MWCNT performed by Raman spectroscopy. MWCNTs are cylindrical nanoparticles combined with multiple graphene layers with their shapes, sizes, and unusual physical properties. In addition, MWCNTs act as a scaffold for the insertion of many metal nanoparticles due to their large surface area^{40–42}. The ratios of I_D/I_G for NiCu@MWCNT nanohybrids and MWCNT were found to be 1.38 and 1.22, respectively. These values show the functionalization and/or defects of multiwalled carbon nanotubes with the help of NiCu nanohybrids. In addition, peak positions of D and G band in the Raman spectrum for NiCu@MWCNT nanohybrid were found as 1,350 and 1,578 cm^{-1} . The XRD pattern of the as-synthesized NiCu@MWCNT catalyst was shown in Fig. S1b. It was observed that the XRD pattern consists of well-separated peaks which indicate a face-centered cubic (fcc) crystal lattice structure. The diffraction peaks detected at 2θ degrees of 42.5°, 61.3°, and 73.5° correspond to planes of (111), (220), and (311), respectively. Furthermore, the peak at 2θ degree of 25.6° (002) specified for MWCNT.

The XPS analysis of the monodisperse NiCu@MWCNT nanohybrids is given in Fig. S2. As shown in Fig. S2a, Cu $2p_{1/2}$, and $2p_{3/2}$ signals can be seen easily and corresponded to the doublets at around 951.6–931.8 and

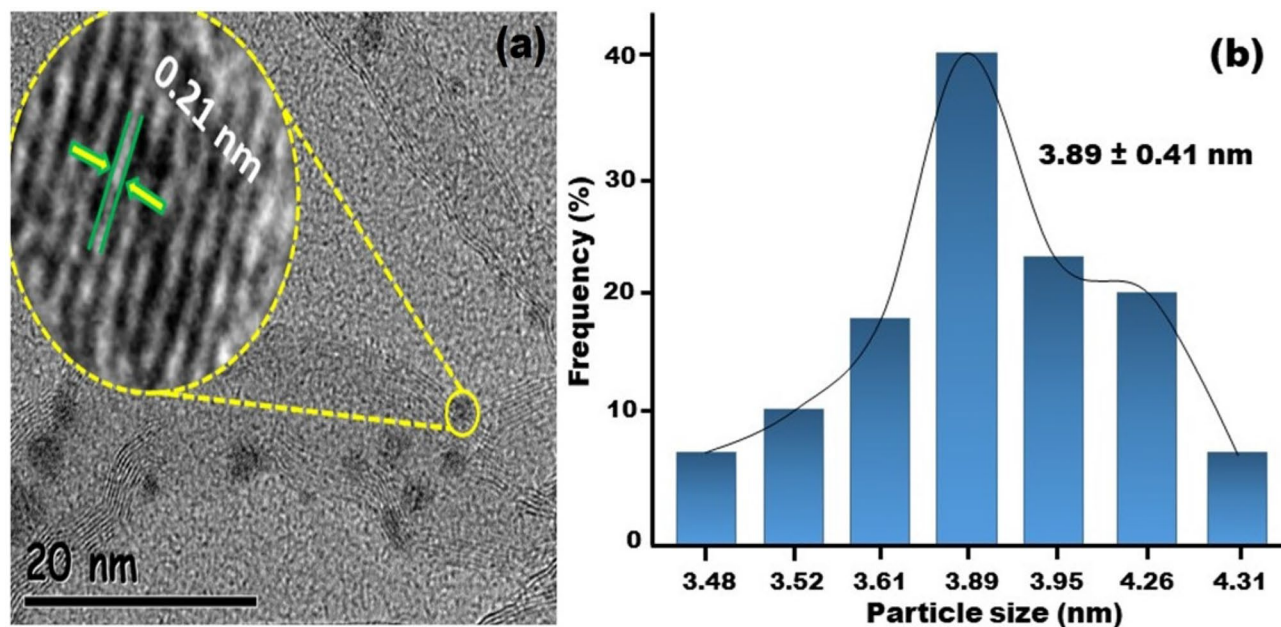


Figure 2. (a) Distribution of NiCu@MWCNT monodisperse TEM and HR-TEM analysis (b) histogram of mean particle size of monodisperse NiCu@MWCNT.

The reaction scheme shows 4-iodobenzaldehyde reacting with malononitrile (1.0 mmol) in the presence of NiCu@MWCNT NPs (1.0 mmol) in a solvent at room temperature (rt) to produce 4-iodobenzylidene malononitrile.

Entry	Solvent	Time (min)	Catalyst (mg)	Yield ^b (%)
1	MeOH	120	4	60 ± 2
2	H ₂ O	120	4	28 ± 3
3	H ₂ O/MeOH (2:1)	30	4	85 ± 2
4	H ₂ O/MeOH (3:1)	30	4	72 ± 1
5	H ₂ O/MeOH (1:1)	25	4	96 ± 3
6	H ₂ O/MeOH (1:1)	240	-	Trace

Table 1. Some solvents and catalysts used for the model reaction of 4-iodobenzaldehyde with malononitrile^a. ^aReaction conditions: 4-iodobenzaldehyde (1.0 mmol), malononitrile (1.0 mmol), NiCu@MWCNT nanohybrids (9.2 wt metal content) and room temperature. ^bIsolated yield.

954.2–934.3 eV, respectively. These values can be ascribed to Cu(II) and Cu(0). Mostly, the formation of Cu(0) and the smaller amount of the formation of Cu(II) were observed. This indicates the formation of NiCu nanohybrids. The smaller amount of Cu(II) most probably comes from some of the unreduced and/or oxidized Cu species. At the same time, the XPS spectra of the Cu 2*p* region show the characteristic shake-up satellites related to CuO and most likely CuO·H₂O arising from the reaction between Cu(II) and the etchant O. The XPS analysis was also examined for Ni 2*p*_{3/2} region which is given in Fig. S2(b) and its core level were found to be 853.2 eV. The reduction of Ni (II) to Ni (0) was occurred during the synthesis process according to the XPS results (Fig. S2b), namely most of the nickel atoms on the surfaces of NiCu@MWCNT nanohybrids have a metallic structure. The other peak at 858.5 eV as shown in Fig. S2(b) shows the formation of a small amount of Ni (II) which is mostly coming from an oxidation or chemical desorption in the catalyst composition during the preparation of the catalyst. After full characterization of monodisperse NiCu@MWCNT nanohybrids, they were performed for Knoevenagel condensation reaction as a model reaction to see the effectiveness of the nanohybrids. Generally, we did not test with solvents outside methanol and water, considering previous work by our group on Knoevenagel condensation. In addition to using methanol and water separately (Table 1, entries 1 and 2), we also used it as a mixture (Table 1, entries 3–6). As can be seen, the water–methanol mixture is more effective in the reaction. The prepared sample containing 4 mg NiCu@MWCNT nanohybrids, 1.0 mmol malononitrile, 1.0 mmol 4-iodobenzaldehyde, and 4 ml solution of water/methanol (v/v = 1/1) gave a very high activity for the

0.033 mmol
NiCu@MW CNT NPs
1.0 mmol CH₂(CN)₂
H₂O/MeOH (1:1), rt

Entry	Substrate	Product	Yield ^b , %	Time (min)	Entry	Substrate	Product	Yield ^b , %	Time (min)
1			96±2	10	8			94±1	18
2			95±1	12	9			95±1	25
3			95±3	15	10			96±3	25
4			95±3	15	11			62±2	40
5			96±1	12	12			92±2	15
6			96±1	12	13			95±2	12
7			74±3	35	14			53±3	180

Table 2. NiCu@MWCNT nanohybrids catalyzed Knoevenagel condensation reaction for different aryl aldehydes and malononitriles^a. ^aReaction conditions: Substrate (1.0 mmol), malononitrile (1.0 mmol) and NiCu@MWCNT (4 mg, 9.2 wt amount of metal) was used with 4 mL of H₂O/CH₃OH (v/v=1/1) at 25 °C. ^bIsolated yield.

Knoevenagel condensation reaction. The results are given in Table 1. No Knoevenagel condensation reaction took place without catalyst.

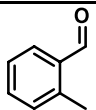
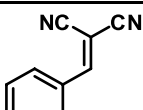
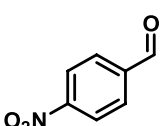
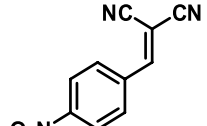
Entry	Substrate	Product	1st		5th	
			Yield ^b (%)	Time (min)	Yield ^b (%)	Time (min)
1			95±3	15	92±1	15
2			96±1	12	93±1	15

Table 3. Reusability performance of NiCu@MWCNT nano hybrids^a. ^aReaction conditions: substrate (1.0 mmol), malononitrile (1.0 mmol) and NiCu@MWCNT nano hybrids (4 mg, %9.2 wt amount of metal), 4 mL of H₂O/CH₃OH (v/v = 1/1) at 25 °C. ^bIsolated yield.

The catalytic efficiency of the NiCu@MWCNT nano hybrids was relatively high compared to that reported in previously published works dealing with the Knoevenagel condensation of benzaldehyde with malononitrile (Table S1).

We tried to summarize all of the aryl and aliphatic aldehydes in Table 2 in conjunction with malononitrile which was successfully used to convert them to BMN compounds by NiCu@MWCNT nano hybrids. Obtaining BMN species at 25 °C in an aqueous solution was carried out quantitatively in 10–180 min. The electron-withdrawing groups linked to the aromatic aldehyde molecules increase the efficiency of the condensation reaction. Table 2, entry 1: 3,4,5-trimethoxybenzaldehyde (1) was converted to 2-(3,4,5-trimethoxybenzylidene) malononitrile (2) with the quantitative yield (96 ± 2%) within 10 min. Table 2, entry 2: 4-hydroxybenzaldehyde (3) was converted to 2-(4-hydroxybenzylidene) malononitrile (4) with quantitative yields (95 ± 1%) within 12 min. Table 2, entry 3, 4: 2-(4-methylbenzylidene) malononitrile (6) and 2-(2-methylbenzylidene) malononitrile (8) were obtained with quantitative yields (95 ± 3%) within 15 min. Although the methoxy, hydroxy, and methyl groups are electron donor groups, the reaction for Table 2 entry 1 was completed earlier (Table 2, entry 2). Methyl groups inductively donate electrons to the aromatic ring. The *ortho* and *para*-toluylaldehyde were converted to the corresponding BMN derivatives with high yields (Table 2, entries 3, 4). 2-(4-nitrobenzylidene) malononitrile (10) and 2-(4-(trifluoromethyl) benzylidene) malononitrile (12) were obtained with a yield of 96 ± 1%. Nitro (-NO₂) and trifluoromethyl (-CF₃) groups are electron-withdrawing groups so that the reactions are completed in a shorter time (Table 2, entries 5, 6).

The *p*-chloro- and iodo benzaldehydes (17 and 19) were respectively converted to 2-(4-chlorobenzylidene) malononitrile (18) and 2-(4-iodobenzylidene) malononitrile (20) with high yields (Table 2, entries 9, 10). But, some changes in reaction time and yield are observed due to the fluorine atom attached to the *para* position. 2-(4-fluorobenzylidene) malononitrile (14) was obtained with a 74 ± 3% yield within 35 min (Table 2, entry 7). There is an overlap agreement between fluorine-carbon due to its *p*-orbital dimensions. This is a known fact. Therefore, compared to other halogen atoms, it is susceptible to electron mesomerically. This reduces the reactivity of the carbonyl group⁴³.

The 2-fluorobenzaldehyde (15) was converted to 2-(2-fluorobenzylidene)malononitrile (16) with a 94 ± 1% yield because of the electronegative effect of the fluorine atom (Table 2, entry 8).

2-(anthracen-9-ylmethylene) malononitrile (22) was successfully synthesized, but with yields lower than the other aryl aldehydes. Moreover, the completion of the process took longer than expected, perhaps due to the steric effect (Table 2, entry 11). The benzaldehyde (23) was converted to 2-benzylidenemalononitrile (24) within 15 min with 92 ± 2% yield (Table 2, entry 12).

2-(2-Furanylmethylene) malononitrile (26) was obtained in quantitative yields and in a short time using furan-2-carbaldehyde (25), which is heteroaromatic aldehyde (Table 2, entry 13). On the other hand, this reaction was carried out with aliphatic aldehydes to compare with aromatic aldehydes. But the major disadvantages in using the aliphatic aldehydes as the starting compound were reaction time and efficiency. 2-Butylidenemalononitrile (28) was obtained with 53 ± 3% yield within 180 min (Table 2, entry 14).

The reusability performance of monodisperse NiCu@MWCNT nano hybrids has also been studied, and it can be seen that monodisperse NiCu@MWCNT nano hybrids retain their initial activity even during the fifth reuse (Table 3).

Conclusions

In conclusion, one-pot, practically, the eco-friendly and recoverable synthetic process has been described for the synthesis of BMN derivatives via Knoevenagel condensation with highly monodisperse NiCu@MWCNT nano hybrids. In the synthesis of NiCu@MWCNT nano hybrids, the new ultrasonic hydroxide assisted reduction method was used, where small monodisperse nano-hybrids were obtained without agglomeration problems. NiCu@MWCNT nano hybrids were identified by Raman spectroscopy, XPS, TEM, HR-TEM, and XRD. All

characterization techniques showed the alloy formation of the NiCu@MWCNT nanohybrids. Monodisperse NiCu@MWCNT nanohybrids displayed an outstanding catalytic performance for the model reaction. The catalytic activity of this system was compared with those of the previous studies and found to be one of the highest performance and the best catalytic efficiency because of the formation of much smaller and the monodisperse nanohybrids on MWCNT with the help of OH- ligands and ultrasonication process. This case can also be explained by the higher stability, larger active chemical surface area, more metallic contents of Ni and Cu, and smaller particle size for the prepared catalyst compared to the others for the model reaction^{43–49}. The obtained NiCu@MWCNT nanohybrids have unique properties such as efficient, safe, economically, and environmentally friendly at room temperature. Due to these distinguishing features, the obtained NiCu@MWCNT nanohybrids will be highly preferred material in future works for the Knoevenagel reaction and will give a new perspective. The effectiveness of the applied method is that it provides a single pot synthesis to facilitate functionalized carbon-based work with MWCNT. This process of heterogeneous catalysts and Knoevenagel condensation is of great importance.

Received: 11 December 2019; Accepted: 20 July 2020

Published online: 29 July 2020

References

- Viel, C. & Doré, J. C. New synthetic cytotoxic and antitumoral agents derived from aristolochic acid, an antitumoral nitrophenanthrenic acid extracted from Aristolochiaceae. *Farmaco. Sci.* **27**, 257–312 (1972).
- Hu, Q. *et al.* Revisiting the Knoevenagel condensations: A universal and flexible bis-ammoniated fiber catalyst for the mild synthesis of α , β -unsaturated compounds. *J. Ind. Eng. Chem.* **54**, 75–81 (2017).
- Maltsev, S. S., Mironov, M. A. & Bakulev, V. A. Synthesis of cyclopentene derivatives by the cyclooligomerization of isocyanides with substituted benzylidenemalononitriles. *Mendeleev Commun.* **16**, 201–202 (2006).
- Sidhu, A., Sharma, J. R., Rai, M. Chemoselective reaction of malononitrile with imine-ones and antifungal potential of products. *Indian J. Chem. Sect. B Org. Med. Chem.* **49**, 247–250 (2010).
- Alwarappan, S., Boyapalle, S., Kumar, A., Li, C.-Z. & Mohapatra, S. Comparative study of single-, few-, and multilayered graphene toward enzyme conjugation and electrochemical response. *J. Phys. Chem. C* **116**, 6556–6559 (2012).
- Khan, S. A. *et al.* Multistep synthesis of fluorine-substituted pyrazolopyrimidine derivatives with higher antibacterial efficacy based on in vitro molecular docking and density functional theory. *J. Heterocycl. Chem.* **54**, 3099–3107 (2017).
- Bhuiyan, M. M. H., Rahman, K. M. M., Alam, M. A. & Mahmud, M. M. Microwave assisted Knoevenagel condensation: Synthesis and antimicrobial activities of some α -cyanoacrylates. *Pakistan J. Sci. Ind. Res. Ser. A Phys. Sci.* **56**, 131–137 (2013).
- Gopalakrishna Panicker, R. K. & Krishnapillai, S. Synthesis of on resin poly(propylene imine) dendrimer and its use as organocatalyst. *Tetrahedron Lett.* **55**, 2352–2354 (2014).
- Almási, M., Zelenák, V., Opanasenko, M. & Čejka, J. A novel nickel metal–organic framework with fluorite-like structure: gas adsorption properties and catalytic activity in Knoevenagel condensation. *Dalt. Trans.* **43**, 3730 (2014).
- Fouda, A. S., El-Ewady, Y. A., Abo-El-Enien, O. M. & Agizah, F. A. Cinnamoylmalononitriles as corrosion inhibitors for mild steel in hydrochloric acid solution. *Anti-Corr. Methods Mater.* **55**, 317–323 (2008).
- Turpaev, K., Ermolenko, M., Cresteil, T. & Drapier, J. C. Benzylidenemalononitrile compounds as activators of cell resistance to oxidative stress and modulators of multiple signaling pathways. A structure–activity relationship study. *Biochem. Pharmacol.* **82**, 535–547 (2011).
- Michel, F. *et al.* The effect of various acrylonitriles and related compounds on prostaglandin biosynthesis. *Prostaglandins* **27**, 69–84 (1984).
- Shahid, M. & Misra, A. A simple and sensitive intramolecular charge transfer fluorescent probe to detect CN⁻ in aqueous media and living cells. *Anal. Methods* **5**, 434–437 (2013).
- Gazit, A., Yaish, P., Gilon, C. & Levitzki, A. Tyrphostins I: synthesis and biological activity of protein tyrosine kinase inhibitors. *J. Med. Chem.* **32**, 2344–2352 (1989).
- Levitzki, A. & Mishani, E. Tyrphostins and other tyrosine kinase inhibitors. *Annu. Rev. Biochem.* **75**, 93–109 (2006).
- Yi, X.-C., Huang, M.-X., Qi, Y. & Gao, E.-Q. Synthesis, structure, luminescence and catalytic properties of cadmium(ii) coordination polymers with 9H-carbazole-2,7-dicarboxylic acid. *Dalt. Trans.* **43**, 3691 (2014).
- Ammar, H. B., Chtourou, M., Frikha, M. H. & Trabelsi, M. Green condensation reaction of aromatic aldehydes with active methylene compounds catalyzed by anion-exchange resin under ultrasound irradiation. *Ultrason. Sonochem.* **22**, 559–564 (2015).
- Bansal, D., Hundal, G. & Gupta, R. A Metalloligand appended with thiazole rings: heterometallic Co³⁺-Zn²⁺ and Co³⁺-Cd²⁺ complexes and their heterogeneous catalytic applications. *Eur. J. Inorg. Chem.* **2015**, 1022–1032 (2015).
- Lolak, N. *et al.* Composites of palladium-nickel alloy nanoparticles and graphene oxide for the Knoevenagel condensation of aldehydes with malononitrile. *ACS Omega* **4**, 6848–6853 (2019).
- Bilgili, H. G. *et al.* Composites of palladium nanoparticles and graphene oxide as a highly active and reusable catalyst for the hydrogenation of nitroarenes. *Microporous Mesoporous Mater.* **296**, 110014 (2020).
- Göksu, H., Burhan, H., Mustafaov, S. D. & Şen, F. Oxidation of benzyl alcohol compounds in the presence of carbon hybrid supported platinum nanoparticles (Pt@CHs) in oxygen atmosphere. *Sci. Rep.* **10**, 5439 (2020).
- Göksu, H., Zengin, N., Burhan, H., Cellat, K. & Şen, F. A novel hydrogenation of nitroarene compounds with multi wall carbon nanotube supported palladium/copper nanoparticles (PdCu@MWCNT NPs) in aqueous medium. *Sci. Rep.* **10**, 8043 (2020).
- Göksu, H. *et al.* Highly efficient and monodisperse graphene oxide furnished Ru/Pd nanoparticles for the dehalogenation of aryl halides via ammonia borane. *ChemistrySelect* **1**, 953–958 (2016).
- Göksu, H., Çelik, B., Yıldız, Y., Şen, F. & Kilbaş, B. Superior monodisperse CNT-supported CoPd (CoPd@CNT) nanoparticles for selective reduction of nitro compounds to primary amines with NaBH₄ in aqueous medium. *ChemistrySelect* **1**, 2366–2372 (2016).
- Göksu, H. *et al.* Eco-friendly hydrogenation of aromatic aldehyde compounds by tandem dehydrogenation of dimethylamineborane in the presence of a reduced graphene oxide furnished platinum nanocatalyst. *Catal. Sci. Technol.* **6**, 2318–2324 (2016).
- Kara, B. Y., Yazici, M., Kilbaş, B. & Gökso, H. A practical and highly efficient reductive dehalogenation of aryl halides using heterogeneous Pd/AlO(OH) nanoparticles and sodium borohydride. *Tetrahedron* **72**, 5898–5902 (2016).
- Pamuk, H., Aday, B., Şen, F. & Kaya, M. Pt NPs@GO as a highly efficient and reusable catalyst for one-pot synthesis of acridinedione derivatives. *RSC Adv.* <https://doi.org/10.1039/c5ra06441d> (2015).
- Mohapatra, S. K., Sonavane, S. U., Jayaram, R. V. & Selvam, P. Heterogeneous catalytic transfer hydrogenation of aromatic nitro and carbonyl compounds over cobalt(II) substituted hexagonal mesoporous aluminophosphate molecular sieves. *Tetrahedron Lett.* **43**, 8527–8529 (2002).

29. Şen, B. *et al.* A novel thiocarbamide functionalized graphene oxide supported bimetallic monodisperse Rh-Pt nanoparticles (RhPt/TC@GO NPs) for Knoevenagel condensation of aryl aldehydes together with malononitrile. *Appl. Catal. B Environ.* **225**, 148–153 (2018).
30. Gao, Z. *et al.* Superparamagnetic mesoporous Mg-Fe bi-metal oxides as efficient magnetic solid-base catalysts for Knoevenagel condensations. *Dalt. Trans.* **39**, 11132 (2010).
31. Zhang, Y. *et al.* Robust Bifunctional lanthanide cluster based metal-organic frameworks (MOFs) for tandem Deacetalization-Knoevenagel reaction. *Inorg. Chem.* **57**, 2193–2198 (2018).
32. Yang, Q., Zhang, H.-Y., Wang, L., Zhang, Y. & Zhao, J. Ru/UiO-66 catalyst for the reduction of nitroarenes and tandem reaction of alcohol oxidation/Knoevenagel condensation. *ACS Omega* **3**, 4199–4212 (2018).
33. Sen, B. *et al.* Composites of palladium-nickel alloy nanoparticles and graphene oxide for the Knoevenagel condensation of aldehydes with malononitrile. *ACS Omega* **4**, 10744–10751 (2019).
34. Diler, F. *et al.* Efficient preparation and application of monodisperse palladium loaded graphene oxide as a reusable and effective heterogeneous catalyst for suzuki cross-coupling reaction. *J. Mol. Liq.* 111967 (2019) doi:10.1016/j.molliq.2019.111967.
35. Sarmah, B. & Srivastava, R. Highly efficient and recyclable basic ionic liquids supported on SBA-15 for the synthesis of substituted styrenes, carbinolamides, and naphthopyrans. *Mol. Catal.* **427**, 62–72 (2017).
36. Farzaneh, F., Kashani Maleki, M. & Rashtizadeh, E. Expedient catalytic access to knoevenagel condensation using Sr3Al2O6 nanocomposite in room temperature. *J. Clust. Sci.* **28**, 3253–3263 (2017).
37. Mu, M., Yan, X., Li, Y. & Chen, L. Post-modified acid-base bifunctional MIL-101(Cr) for one-pot deacetalization-Knoevenagel reaction. *J. Nanoparticle Res.* **19**, 148 (2017).
38. de Resende Filho, J. B. M., Pires, G. P., de Oliveira Ferreira, J. M. G., Teotonio, E. E. S. & Vale, J. A. Knoevenagel Condensation of Aldehydes and Ketones with Malononitrile Catalyzed by Amine Compounds-Tethered Fe3O4@SiO2 Nanoparticles. *Catal. Letters* **147**, 167–180 (2017).
39. Rambabu, D., Ashraf, M., Pooja, G. A. & Dhir, A. Mn-MOF@Pi composite: synthesis, characterisation and an efficient catalyst for the Knoevenagel condensation reaction. *Tetrahedron Lett.* **58**, 4691–4694 (2017).
40. Tong, Y., Boldoo, T., Ham, J. & Cho, H. Improvement of photo-thermal energy conversion performance of MWCNT/Fe3O4 hybrid nanofluid compared to Fe3O4 nanofluid. *Energy* **196**, 117086 (2020).
41. Gangu, K. K., Maddila, S. & Jonnalagadda, S. B. A review on novel composites of MWCNTs mediated semiconducting materials as photocatalysts in water treatment. *Sci. Total Environ.* **646**, 1398–1412 (2019).
42. Naghadeh, S. B., Vahdatifar, S., Mortazavi, Y., Khodadadi, A. A. & Abbasi, A. Functionalized MWCNTs effects on dramatic enhancement of MWCNTs/SnO2 nanocomposite gas sensing properties at low temperatures. *Sens. Actuators B Chem.* **223**, 252–260 (2016).
43. Holl, M. G., Struble, M. D., Singal, P., Siegler, M. A. & Lectka, T. Positioning a carbon-fluorine bond over the π cloud of an aromatic ring: a different type of arene activation. *Angew. Chemie Int. Ed.* **55**, 8266–8269 (2016).
44. Viswanadham, B., Jhansi, P., Chary, K. V. R., Friedrich, H. B. & Singh, S. Efficient solvent free knoevenagel condensation over vanadium containing heteropolyacid catalysts. *Catal. Letters* **146**, 364–372 (2016).
45. Taher, A., Lee, D.-J., Lee, B.-K. & Lee, I.-M. Amine-functionalized metal-organic frameworks: an efficient and recyclable heterogeneous catalyst for the Knoevenagel condensation reaction. *Synlett* **27**, 1433–1437 (2016).
46. Sakthivel, B. & Dhakshinamoorthy, A. Chitosan as a reusable solid base catalyst for Knoevenagel condensation reaction. *J. Colloid Interface Sci.* **485**, 75–80 (2017).
47. Martínez, F., Orcajo, G., Briones, D., Leo, P. & Calleja, G. Catalytic advantages of NH2-modified MIL-53(Al) materials for Knoevenagel condensation reaction. *Microporous Mesoporous Mater.* **246**, 43–50 (2017).
48. Göksu, H. & Gültekin, E. Pd nanoparticles incarcerated in aluminium oxy-hydroxide: an efficient and recyclable heterogeneous catalyst for selective Knoevenagel condensation. *ChemistrySelect* **2**, 458–463 (2017).
49. Ezugwu, C. I., Mousavi, B., Asraf, M. A., Luo, Z. & Verpoort, F. Post-synthetic modified MOF for Sonogashira cross-coupling and Knoevenagel condensation reactions. *J. Catal.* **344**, 445–454 (2016).

Acknowledgements

The authors would like to thank Dumlupinar University (2014–05, 2015–35, and 2015–50) and Duzce University (grant no. 2015.26.04.371) for funding.

Author contributions

H.G. and F.S. organized all experiments and wrote the manuscript. N.Z., H.B. and A.S. performed all experiments and characterizations. They have also drawn the figures.

Competing interests

The authors declare no competing interests.

Additional information

Supplementary information is available for this paper at <https://doi.org/10.1038/s41598-020-69764-8>.

Correspondence and requests for materials should be addressed to H.G. or F.Ş.

Reprints and permissions information is available at www.nature.com/reprints.

Publisher's note Springer Nature remains neutral with regard to jurisdictional claims in published maps and institutional affiliations.



Open Access This article is licensed under a Creative Commons Attribution 4.0 International License, which permits use, sharing, adaptation, distribution and reproduction in any medium or format, as long as you give appropriate credit to the original author(s) and the source, provide a link to the Creative Commons license, and indicate if changes were made. The images or other third party material in this article are included in the article's Creative Commons license, unless indicated otherwise in a credit line to the material. If material is not included in the article's Creative Commons license and your intended use is not permitted by statutory regulation or exceeds the permitted use, you will need to obtain permission directly from the copyright holder. To view a copy of this license, visit <http://creativecommons.org/licenses/by/4.0/>.

© The Author(s) 2020